

Effect of nonlinear filters on detrended fluctuation analysis

Zhi Chen,¹ Kun Hu,¹ Pedro Carpena,² Pedro Bernaola-Galvan,² H. Eugene Stanley,¹ and Plamen Ch. Ivanov¹

¹*Center for Polymer Studies and Department of Physics,
Boston University, Boston, Massachusetts 02215*

²*Departamento de Física Aplicada II, ETSI de Telecomunicación, Universidad de Málaga, Spain*

(Dated: October 27, 2018)

When investigating the dynamical properties of complex multiple-component physical and physiological systems, it is often the case that the measurable system's output does not directly represent the quantity we want to probe in order to understand the underlying mechanisms. Instead, the output signal is often a linear or nonlinear function of the quantity of interest. Here, we investigate how various linear and nonlinear transformations affect the correlation and scaling properties of a signal, using the detrended fluctuation analysis (DFA) which has been shown to accurately quantify power-law correlations in nonstationary signals. Specifically, we study the effect of three types of transforms: (i) linear ($y_i = ax_i + b$); (ii) nonlinear polynomial ($y_i = ax_i^k$); and (iii) nonlinear logarithmic [$y_i = \log(x_i + \Delta)$] filters. We compare the correlation and scaling properties of signals before and after the transform. We find that linear filters do not change the correlation properties, while the effect of nonlinear polynomial and logarithmic filters strongly depends on (a) the strength of correlations in the original signal, (b) the power k of the polynomial filter, and (c) the offset Δ in the logarithmic filter. We further apply the DFA method to investigate the "apparent" scaling of three analytic functions: (i) exponential [$\exp(\pm x + a)$], (ii) logarithmic [$\log(x + a)$], and (iii) power law [$(x + a)^\lambda$], which are often encountered as trends in physical and biological processes. While these three functions have different characteristics, we find that there is a broad range of values for parameter a common for all three functions, where the slope of the DFA curves is identical. We further note that the DFA results obtained for a class of other analytic functions can be reduced to these three typical cases. We systematically test the performance of the DFA method when estimating long-range power-law correlations in the output signals for different parameter values in the three types of filters and the three analytic functions we consider.

PACS numbers: 05.40.-a

I. INTRODUCTION

Many physical and biological systems under multi-component control mechanisms exhibit scale-invariant features characterized by long-range power-law correlations in their output. These scaling features are often difficult to quantify due to the presence of erratic fluctuations, heterogeneity, and nonstationarity embedded in the output signals. This problem becomes even more difficult in certain cases: (i) when we cannot probe directly the quantity of interest in experimental settings, i.e., the measurable output signal is a linear or nonlinear function of the quantity of interest; (ii) when measuring devices impose a linear or nonlinear filter on the system's output; (iii) when we are interested not in the output signal but in a specific component of it, which is obtained through a nonlinear transform (e.g., the magnitude or the sign of the fluctuations in the signal); (iv) when comparing the dynamics of different systems by applying nonlinear transforms to their output signals; or (v) when pre-processing the output signal by means of linear or nonlinear filters before the actual analysis. Thus, to understand the intrinsic dynamics of a system, in such cases it is important to correctly analyze and interpret the dynamical patterns in the system's output.

Conventional two-point correlation, power spectrum, and Hurst analysis methods are not suited for nonstationary signals, the statistical properties of which change

with time [1, 2, 3]. To address this problem, detrended fluctuation analysis (DFA) method was developed to accurately quantify long-range correlations embedded in a nonstationary time series [4, 5]. This method provides a single quantitative parameter — the scaling exponent α — to quantify the scale-invariant properties of a signal. One advantage of the DFA method is that it allows the detection of long-range power-law correlations in noisy signals with embedded polynomial trends that can mask the true correlations in the fluctuations of a signal. Recent comparative studies have demonstrated that the DFA method outperforms conventional techniques in accurately quantifying correlation properties over a wide range of scales [6, 7, 8, 9, 10]. The DFA method has been widely applied to DNA [4, 6, 7, 11, 12, 13], cardiac dynamics [14, 15, 16, 17, 18, 19, 20, 21, 22, 23, 24, 25, 26, 27, 28, 29, 30], human electroencephalographic (EEG) fluctuations [31], human motor activity [32] and gait [33, 34, 35, 36, 37], meteorology [38, 39], climate temperature fluctuations [40, 41, 42, 43, 44, 45], river flow and discharge [46, 47], electric signals [48, 49, 50], stellar x-ray binary systems [51], neural receptors in biological systems [52], music [53], and economics [54, 55, 56, 57, 58, 59, 60, 61]. In many of these applications the main problem is to differentiate scaling features in a system's output which are inherent to the underlying dynamics, from the scaling features which are an artifact of nonstationarities or different types of transforms and

filters.

In two previous studies we have examined how different types of nonstationarities such as superposed sinusoidal and power-law trends, random spikes, cut-out segments, and patches with different local behavior affect the long-range correlation properties of signals [10, 62]. Here we use the DFA method to investigate how the scaling properties of noisy correlated signals change under linear and nonlinear transforms. Further, (i) we test to see under what types of transforms (filters) it is possible to derive information about the scaling properties of the signal of interest before the transformation, provided we know the correlation behavior of the transformed (filtered) signal, and (ii) we probe the “apparent” scaling of three common transformation functions after applying the DFA method — exponential, logarithmic and polynomial. We also evaluate the limitations of the DFA method under linear and nonlinear transforms. Specifically, we consider the following:

(1) *Correlation properties of signals after transforms of the type:* $\{x_i\} \implies \{f(x_i)\}$, where $\{x_i\}$ is a stationary signal with *a priori* known correlation properties.

(i) *Linear transform:* $\{x_i\} \implies \{ax_i + b\}$. Transforms of this type are often encountered in physical systems. For example: (a) from the fluctuations in the acceleration of a particle (measurable quantity), one can derive information about how the force (quantity of interest) acting on this particle changes in time without directly measuring the force: $\{a(t_i)\} \implies \{F(t_i) = ma(t_i)\}$; (b) in pnp-transistors a difficult to directly measure base (input) current I_B (quantity of interest) is amplified hundreds of times, so that small fluctuations in I_B may lead to significant (and measurable) changes in the collector (output) signal I_C (measurable quantity): $\{I_C(t_i)\} \implies \{I_B(t_i) = I_C(t_i)/\beta\}$, and (c) changes in the volume V (quantity of interest) of an ideal gas can be determined from fluctuations in the temperature (measurable quantity) provided the pressure is kept constant: $\{T(t_i)\} \implies \{V(t_i) = \frac{nR}{P}T(t_i)\}$.

(ii) *Nonlinear polynomial transform:* $\{x_i\} \implies \{ax_i^k\}$, where $k \neq 1$ and takes on positive integer values. For example: (a) from fluctuations in the current I (measurable quantity) one can extract information about the behavior of the power lost as heat P (quantity of interest) in a resistor: $\{I(t_i)\} \implies \{P(t_i) = RI^2(t_i)\}$; (b) measuring the temperature T fluctuations of a radiating body the Stefan’s law defines the power emitted per unit area: $\{T_i\} \implies \{\epsilon_i = \sigma T_i^4\}$. Further, linear and nonlinear polynomial filters are also used to renormalize data series representing an identical quantity measured in different systems before performing correlation analysis, e.g., (i) normalizing heart rate recordings from different subjects to zero mean and unit standard deviation (linear filters), or (ii) extracting the absolute value (nonlinear filter) of the heartbeat fluctuations in datasets obtained from different subjects [25].

In this study we consider two examples of nonlinear polynomial filters — quadratic and cubic filters — which

represent the class of polynomial filters with even and odd powers, and we investigate how these filters change the correlation properties of signals. Since polynomial filters with even power wipe out the sign information in a signal, we expect quadratic and cubic filters to have a different effect. A recent study by Y. Ashkenazy *et al.* [25] shows that the magnitude of a signal (without sign information) exhibits different correlation properties from that of the original signal. Thus it is necessary to investigate how quadratic and cubic filters change the scaling properties of correlated signals.

(iii) *Logarithmic filter:* $\{x_i\} \implies \{\log(x_i + \Delta)\}$, is also widely used in renormalizing datasets obtained from different sources before comparative analysis. For example, to compare the dynamics of price fluctuations $X(i)$ of different company stocks, which may have a different average price, one often first obtains the relative price returns $R(i) = \log[X(i+1)/X(i)]$ before performing correlation analysis [55, 63]. It is assumed that upon taking the returns one does not alter the information contained in the original signal. To test this assumption we compare the correlation properties of the signal before and after a logarithmic filter.

(2) *Correlation properties of transformation functions*

When analyzing the correlation properties of a signal after a given transform, it may be valuable to know what is the DFA result for the transformation function itself. In addition, it is often the case that noisy signals are superposed on trends which can be approximated by a certain function. Previous studies have demonstrated that the DFA result of a correlated signal with a superposed trend is a superposition of the DFA result for the signal and the DFA result for the analytic function representing the trend [10, 62]. Here we investigate separately the results of the DFA for three functions which are very often encountered in physical and biological processes: (i) *exponential*, (ii) *logarithmic* and (iii) *power law*.

The layout of this paper is as follows: In Sec. II, we describe how we generate signals with desired long-range power-law correlations and introduce the DFA method used to quantify correlations in nonstationary signals. In Sec. III, we compare the correlation and scaling properties of signals before and after linear and nonlinear polynomial transforms. In Sec. IV, we consider the effect of nonlinear logarithmic filter on the long-range correlation properties of stationary signals. In Sec. V, we investigate the performance of the DFA method on three analytic functions — exponential, logarithmic, and power-law — which are often encountered as trends in physical and biological time series. We systematically examine the crossovers in the scaling behavior of correlated signals resulting from the transforms and trends discussed in Secs. III-V, the conditions of existence of these crossovers and their typical characteristics. We summarize our findings in Sec. VI.

II. METHODS

We analyze two types of signals:

(1) stochastic stationary signals $\{x_i\}$ ($i = 1, 2, 3, \dots, N_{\max}$) with different type of correlations (uncorrelated, correlated, and anti-correlated) and surrogate signals obtained from $\{x_i\}$ after linear and nonlinear transforms. We use an algorithm based on the Fourier transform to generate stationary signals $\{x_i\}$ with long-range power-law correlations as described in [62, 64, 65]. The generated signals $\{x_i\}$ have zero mean and unit standard deviation.

(2) Exponential, logarithmic, and power-law functions which often represent transformations or trends in physical and biological data.

We use the detrended fluctuation analysis (DFA) method [6, 7] to quantify the correlation and scaling properties of these signals. The DFA method is described in detail elsewhere [10, 62]. Briefly, it involves the following steps: (i) we integrate the signal after subtracting the global average; (ii) we then divide the time series into boxes of length n and perform, in each box, a least-square polynomial fit of order ℓ to the integrated signal to remove the local trend in each box; (iii) in each box we calculate the root-mean-square fluctuation function $F(n)$ quantifying the fluctuations of the integrated signal along the local trend; (iv) we repeat this procedure for different box sizes (time scales) n .

A power-law relation between the average root-mean-square fluctuation function $F(n)$ and the box size n indicates the presence of scaling: $F(n) \sim n^\alpha$. The scale n for which this scaling holds represents the length of the correlation. The fluctuations in a signal can be characterized by the scaling exponent α , a self-similarity parameter which quantifies the strength of the long-range power-law correlations in the signal. If $\alpha = 0.5$, there is no correlation and the signal is uncorrelated (white noise); if $\alpha < 0.5$, the signal is anti-correlated; if $\alpha > 0.5$, the signal is correlated. Since we use a polynomial fit of order ℓ , we denote the algorithm as DFA- ℓ . Further, we note that for stationary signals $\{x_i\}$ with long-range power-law correlations, the value of the scaling exponent α is related to the exponent β in the power spectrum $S(f) = f^{-\beta}$ of signals $\{x_i\}$ by $\beta = 2\alpha - 1$ [6]. Since the power spectrum is the Fourier transform of the autocorrelation function, one can find the following relationship between the autocorrelation exponent γ and the power spectrum exponent β : $\gamma = 1 - \beta = 2 - 2\alpha$, where γ is defined by the autocorrelation function $C(\tau) = \tau^{-\gamma}$ and should satisfy $0 < \gamma < 1$ [9].

The upper threshold for the value of the scaling exponent α is related to the order ℓ of the DFA method: $\alpha \leq \ell + 1$ for DFA- ℓ [10]. In addition, integrating the signal before applying the DFA method will increase the value of the scaling exponent α by 1, thus the upper threshold will become $\alpha + 1 \leq \ell + 1$ for DFA- ℓ . Therefore, after integrating correlated signals with the scaling exponent $\alpha > \ell$, one needs to apply the DFA method with an

order of polynomial fit higher than ℓ . We also note that for anti-correlated signals, the scaling exponent obtained from the DFA- ℓ method overestimates the true correlations at small scales [10]. To avoid this problem, one needs first to integrate the original anti-correlated signal and then to apply the DFA- ℓ method [10, 62]. The correct scaling exponent α can then be obtained from $F(n)/n$ [instead of $F(n)$] [10, 25, 62]. For that reason we first integrate and then apply the DFA method when considering anti-correlated signals.

III. EFFECTS OF LINEAR AND NONLINEAR POLYNOMIAL TRANSFORMS

In this section, we study the effect of linear and nonlinear polynomial transforms (filters) on the scaling properties of stationary signals $\{x_i\}$ with long-range power-law correlations. Specifically, we consider two types of nonlinear transforms — quadratic and cubic — as an example of even and odd polynomial filters. We generate the signals $\{x_i\}$ with linear fractal properties and with *a priori* build-in correlations characterized by a DFA scaling exponent α [4, 10, 62]. We compare how the exponent α changes after the transform.

We first test to see if these transforms affect the properties of uncorrelated signals (white noise). We find that the linear, quadratic, and cubic filters do not change the scaling properties of white noise — the curves of the detrended fluctuation function $F(n)$ for the filtered signals $\{f(x_i)\}$ collapse on the scaling curve of the original signal $\{x_i\}$, and the scaling exponent $\alpha = 0.5$ remains unchanged [Fig. 1(a)].

For signals with correlations we find that the linear and nonlinear polynomial filters have a different effect. In particular, for both correlated ($\alpha > 0.5$) and anti-correlated ($\alpha < 0.5$) signals $\{x_i\}$ we find that the scaling properties remain unchanged after the linear filter. In contrast, the quadratic and cubic filters change the scaling behavior of both correlated and anti-correlated signals [Fig. 1(b-d)]. Specifically, for *anti-correlated* signals, we find that: (i) after the quadratic filter the scaling behavior is dramatically changed to uncorrelated (random) behavior with $\alpha = 0.5$ at all scales; (ii) after the cubic filter the scaling (correlation) function $F(n)$ of anti-correlated signals is also changed and exhibits a crossover from anti-correlated behavior at small scales to uncorrelated behavior at larger scales [Fig. 1(b)]. We note that the quadratic filter removes the sign information in a signal, thus completely eliminating the anti-correlations in a signal. In contrast, the effect of the cubic filter is not as strong as the effect of the quadratic filters, since a cubic filter preserves the sign information and the anti-correlations at small scales. For *correlated* signals we find that after both quadratic and cubic filters, the scaling behavior is unchanged at small and intermediate scales. At large scales we observe a crossover to weaker correlations which is less pronounced when increasing the strength of

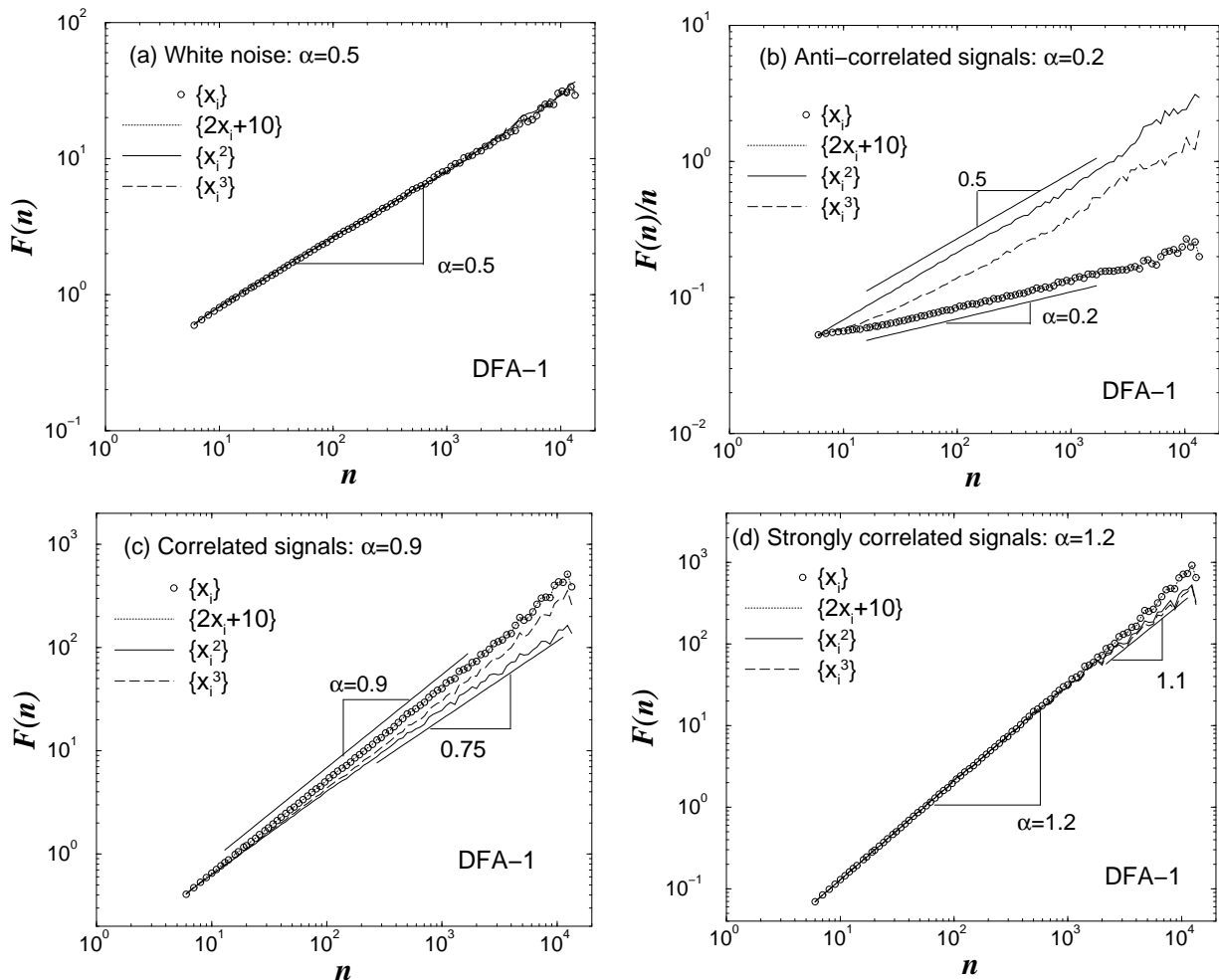


FIG. 1: Effects of linear, quadratic, and cubic filters on the scaling behavior of long-range correlated stationary, Gaussian distributed (zero mean and unit standard deviation) signals $\{x_i\}$: (a) uncorrelated, (b) anti-correlated, (c) correlated, and (d) strongly correlated. The length of each signal is $N_{max} = 2^{17}$. In our analysis we use the DFA-1 method. The curves of the detrended fluctuation function $F(n)$ for all signals are vertically shifted so that they start at the same value of $F(n)$ at the minimal scale n . For anti-correlated signals we first integrate and then apply the DFA-1 method to avoid overestimation of the true correlations at small scales due to limitations of the DFA method ([10, 62] and Sec. II). Our analysis shows that after a linear filter the scaling behavior remains unchanged. In contrast, nonlinear polynomial filters change the scaling behavior of anti-correlated and correlated signals, leading to crossovers at large scales.

the correlations (higher values of α) in the signal $\{x_i\}$ [Fig. 1(c-d)]. For signals with very strong correlations ($\alpha > 1$), we find that the scaling behavior remains almost unchanged after nonlinear polynomial filters. We also find that the quadratic filter leads to a more pronounced crossover at large scales compared to the cubic filter for all positively correlated signals.

IV. LOGARITHMIC FILTER

In addition to nonlinear polynomial transforms, logarithmic transforms are often used in preprocessing procedures when there is a need to renormalize output signals obtained from different systems before comparing their correlation properties [55]. In this section, we investigate

the effect of logarithmic filters on the scaling properties of stationary signals with long-range power-law correlations.

We first generate stationary correlated signals $\{x_i\}$ with a zero mean and unit standard deviation, and with *a priori* known and controlled correlation properties quantified by DFA scaling exponent α . To ensure that all values in the signal are positive, before the logarithmic transform, we shift $\{x_i\} \Rightarrow \{x_i + \Delta\}$, where $\Delta = -x_{min} + \epsilon$, x_{min} is the minimal value in the series $\{x_i\}$ and ϵ is a positive constant. This linear transform does not alter the correlation properties of $\{x_i\}$, as demonstrated in Sec. III, Fig. 1. Next we integrate the signal after the logarithmic transform $\{\log_{10}(x_i - x_{min} + \epsilon)\}$ and we perform a DFA-2 analysis.

For uncorrelated (white noise) signals after the loga-

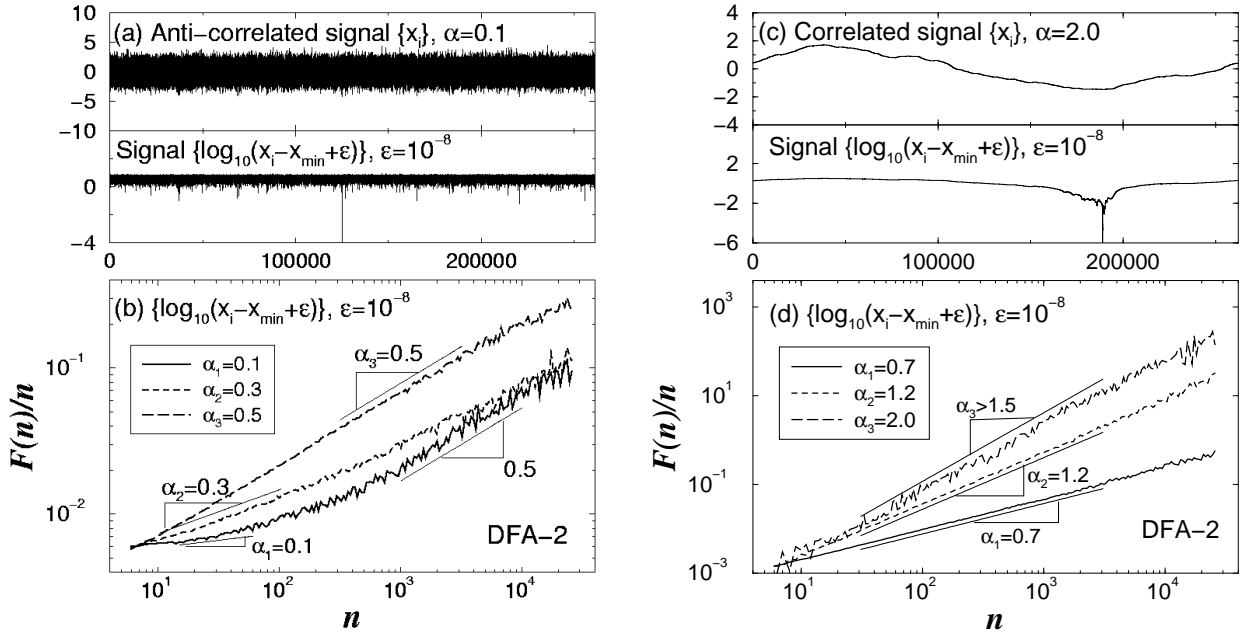


FIG. 2: Effects of the nonlinear logarithmic filter $\{\log_{10}(x_i - x_{min} + \epsilon)\}$ on the scaling behavior of stationary correlated signals $\{x_i\}$, where x_{min} is the minimal value in the original signal $\{x_i\}$ and ϵ is a positive constant. The original signals $\{x_i\}$ have zero mean, unit standard deviation, and length $N_{max} = 2^{18}$. (a) Original strongly anti-correlated signal $\{x_i\}$ with DFA correlation exponent $\alpha = 0.1$ and the corresponding signal after logarithmic filter. (b) DFA scaling curves $F(n)$ for anti-correlated signals and white noise after the logarithmic filter show a crossover to “white noise” behavior (i.e., slope= 0.5) at large scales. To obtain more accurate scaling, we first integrate the signal $\{\log_{10}(x_i - x_{min} + \epsilon)\}$ and then apply DFA-2 method (see Sec. II). (c) Original strongly correlated signal $\{x_i\}$ with the DFA correlation exponent $\alpha = 2$ and the corresponding signal after logarithmic filter. (d) DFA scaling curves for correlated signals $\{x_i\}$ after the logarithmic filter. We find that the logarithmic filter does not change the correlation properties of signals with certain positive correlations (e.g., $\alpha = 0.7$ and $\alpha = 1.2$), though it weakens the correlations in signals with very strong positive correlations (e.g., $\alpha = 2$).

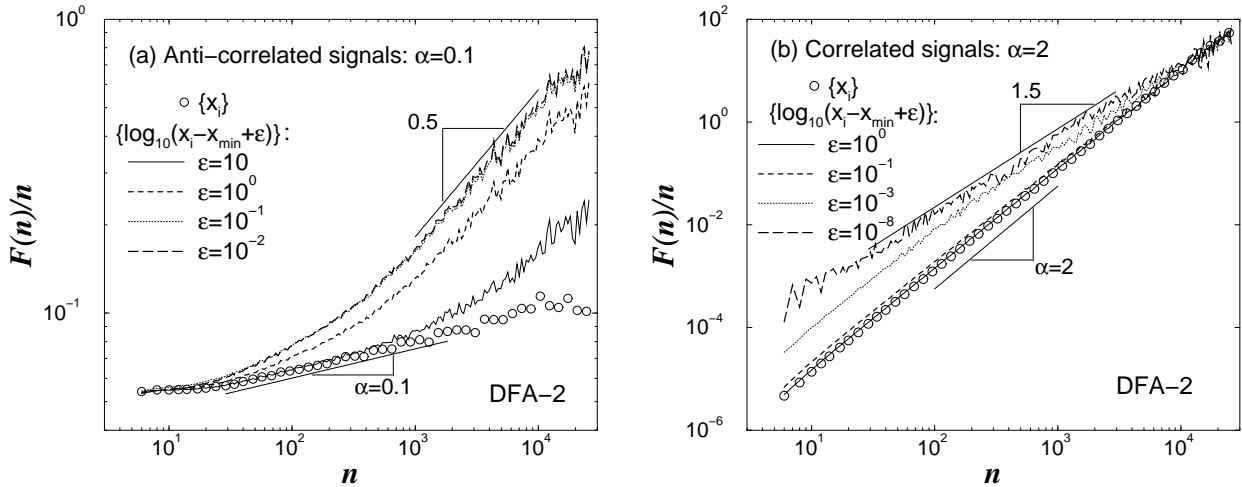


FIG. 3: Dependence of the effect of logarithmic filter $\{\log_{10}(x_i - x_{min} + \epsilon)\}$ on the offset parameter ϵ . (a) Detrended fluctuation function $F(n)$ from the DFA-2 after integration of $\{\log_{10}(x_i - x_{min} + \epsilon)\}$, for an anti-correlated signal with the DFA correlation exponent $\alpha = 0.1$ and varied values of ϵ . We find that for smaller values of ϵ , there is a more pronounced crossover to uncorrelated behavior with $\alpha = 0.5$. (b) Detrended fluctuation function $F(n)$ from the DFA-2 after integration of $\{\log_{10}(x_i - x_{min} + \epsilon)\}$, for a signal with strong positive correlations ($\alpha = 2$) and varied values of ϵ . We find that signals with strong positive correlations are less affected by the logarithmic filter compared to the anti-correlated signals in (a) and that for smaller values of ϵ , there is a more pronounced crossover.

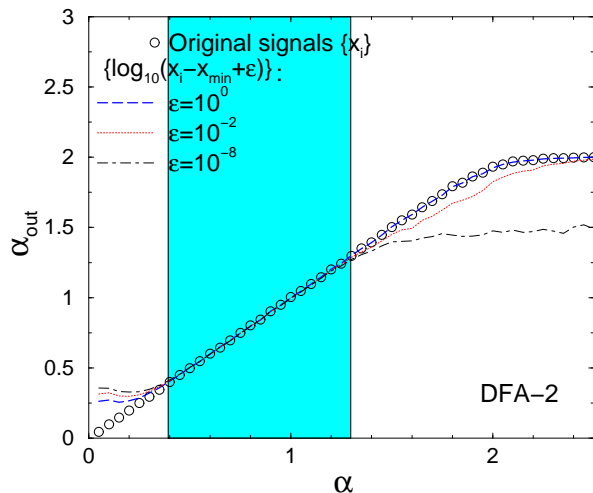


FIG. 4: Relation between the scaling exponent α of the original “input” stationary signals and the correlation exponent α_{out} of the signals after the logarithmic filter $\{\log(x_i - x_{min} + \epsilon)\}$, where x_{min} is the minimal value in the original signal $\{x_i\}$ and ϵ is a positive constant. α_{out} is obtained from the DFA-2 analysis after integrating the signal $\{\log(x_i - x_{min} + \epsilon)\}$ and fitting the detrended fluctuation function $F(n)$ in the region $n \in [30, 3000]$. Our results show that for signals with a correlation exponent α outside the shaded region, the logarithmic filter changes the scaling behavior ($\alpha_{out} \neq \alpha$) and this change depends on the offset parameter ϵ .

rithmic filter, we find no change in the scaling properties and the correlation exponent remains $\alpha = 0.5$ in the entire range of scales [Fig. 2(b)]. However, we find that the scaling properties of signals with certain degree of correlation change significantly. Specifically, for anti-correlated signals ($\alpha < 0.5$) we observe a crossover to uncorrelated (white noise) behavior at large scales. This crossover becomes more pronounced (and shifted to smaller scales) when increasing the strength of anti-correlations (decreasing α) [Fig. 2(b)]. This crossover behavior is caused by negative spikes in the signal following the logarithmic transform [Fig. 2(a)]. A similar effect was previously reported for stationary correlated signals with superposed random spikes [62]. For correlated signals ($\alpha > 0.5$), we find a threshold value for the correlation exponent $\alpha_{th} \approx 1.3$, below which the scaling properties of the signal remain unchanged after the logarithmic filter. Above α_{th} there is a reduction in the strength of the positive correlations, i.e., the value of the estimated exponent after the logarithmic filter is much lower compared to the correlation exponent α in the original signal [Fig. 2(d)].

Since the logarithmic filter is a nonlinear transform which diverges for values of the signal $\{x_i - x_{min} + \epsilon\}$ close to zero, we next test how the scaling properties of the signal depend on the value of the offset parameter ϵ . We consider anti-correlated and correlated signals with fixed values of α and varied ϵ . For strongly anti-correlated signals we find that even for large values of ϵ ,

there is a crossover to uncorrelated behavior in the scaling curve $F(n)$ at large scales (note that ϵ is the minimal value of the signal $\{x_i - x_{min} + \epsilon\}$). This crossover shifts to smaller scales with decreasing ϵ [Fig.3(a)]. Further, we find that for decreasing ϵ , the scaling curves $F(n)$ converge to a single curve, indicating random uncorrelated behavior in the range of large and intermediate scales. For anti-correlated signals with $\alpha = 0.1$ we find that this convergence is reached for $\epsilon < 0.1$ [Fig.3(a)]. For signals with strong positive correlations ($\alpha > \alpha_{th}$), we also observe a change in the scaling behavior which becomes more pronounced when ϵ decreases. However, in contrast to the anti-correlated signals, the deviation from the expected accurate scaling starts at intermediate scales and extends to smaller scales with decreasing ϵ [Fig.3(b)]. For signals with very strong correlations, e.g. $\alpha = 2$, the deviation from the accurate scaling is observed only for $\epsilon < 0.1$, while for $\epsilon > 0.1$, there is no effect on the scaling [Fig.3(b)]. This is in contrast to the situation observed for signals with strong anti-correlations ($\alpha = 0.1$) where the logarithmic filter alters the scaling behavior even for much larger values $\epsilon > 10$ [Fig.3(a)].

Finally we study the relation between the scaling exponent α of the original “input” signal and the estimated exponent α_{out} of the “output” signal after the logarithmic filter. We find that for correlated signals within given range for the value of the scaling exponent $\alpha \in [0.4, 1.3]$, there is no change in the scaling properties after the logarithmic transform. However, for signals with correlation exponents $\alpha < 0.4$ and $\alpha > 1.3$, we find that the logarithmic transform can dramatically change the scaling behavior and this effect also strongly depends on the value of the offset parameter ϵ [Fig.4]. Therefore, the logarithmic filter is not recommended for anti-correlated signals and signals with very strong positive correlations — applying this filter will mask the true correlations in the original signals.

V. RESULTS OF THE DFA FOR TRANSFORMATION FUNCTIONS

In this section we investigate the scaling properties of three functions: *exponential*, *logarithmic*, and *power-law*. These functions are often used in signal processing as transforms of various stochastic correlated signals and also appear as trends superposed on noisy signals derived from physical and biological systems. In previous work [10, 62] we have demonstrated that the scaling behavior of a correlated signal with a superposed trend is superposition of the scaling behavior of the correlated signal and the “apparent” scaling behavior obtained from the DFA method for the analytic function representing the trend. Therefore, understanding the results of the DFA for certain analytic functions becomes a necessary step to quantify the scaling behavior of system’s outputs where correlated fluctuations are superposed with different trends.

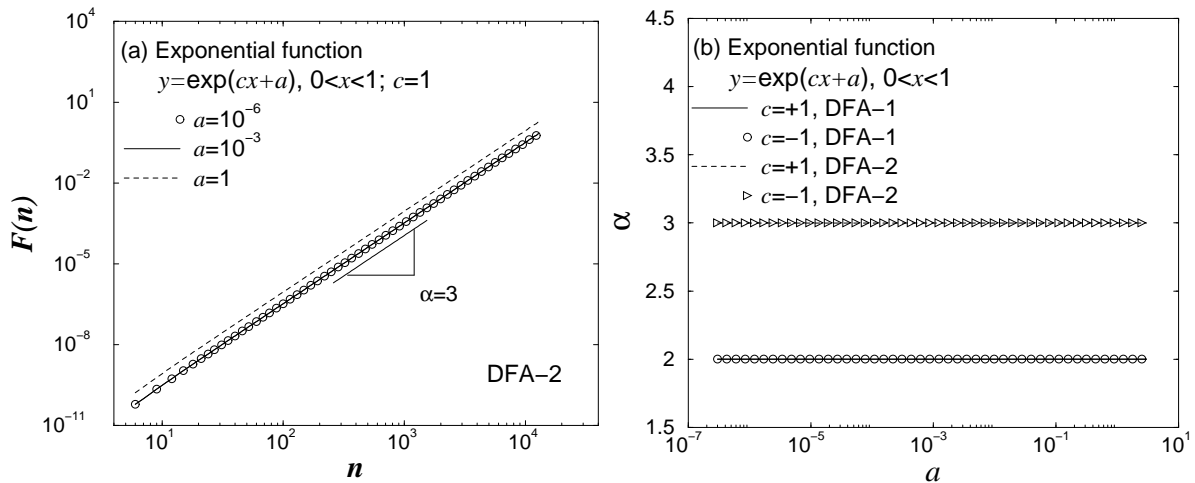


FIG. 5: The results of the DFA method for general exponential function: $y = \exp(cx + a)$, $0 < x \leq 1$, $x = i/N_{max}$, $i = 1, 2, \dots, N_{max}$, $N_{max} = 2^{17}$, where $c = \pm 1$ and offset a is a positive constant. (a) Detrended fluctuation function $F(n)$ obtained using the DFA-2 method for different values of the offset parameter a . While there is a vertical shift in $F(n)$ for different values of a , all scaling curves are characterized by an identical slope α . (b) Dependence of the scaling exponent α on the parameters a and c . We find that for any exponential function the scaling exponent α depends only on the order ℓ of the DFA method: $\alpha = \ell + 1$.

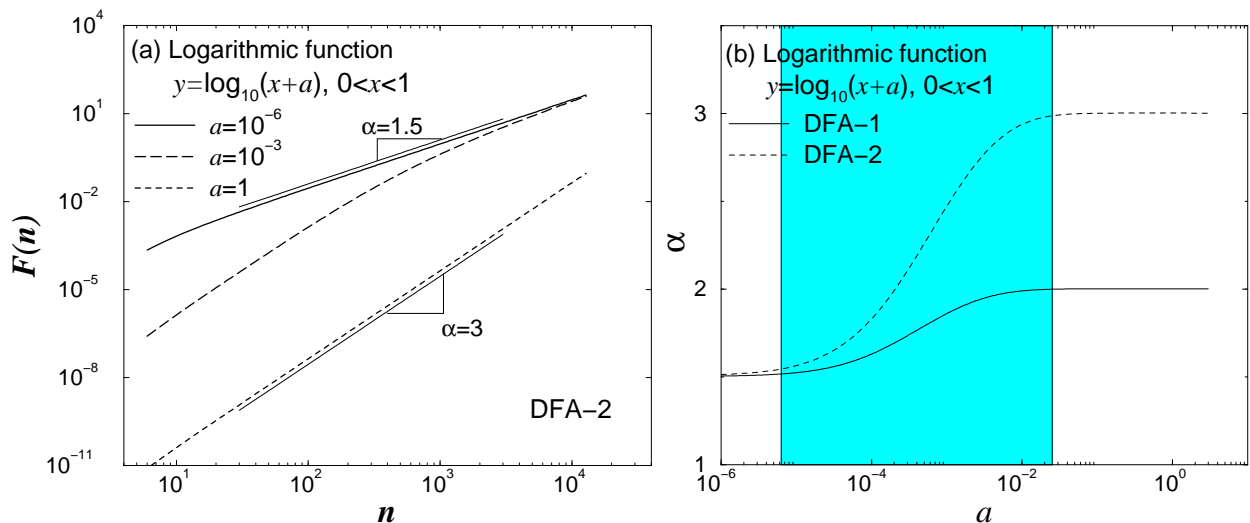


FIG. 6: The results of the DFA method for general logarithmic function $y = \log_{10}(x + a)$, $0 < x \leq 1$, $x = i/N_{max}$, $i = 1, 2, \dots, N_{max}$, $N_{max} = 2^{17}$, where offset a is a positive constant. (a) Detrended fluctuation function $F(n)$ obtained using the DFA-2 method for different values of the offset parameter a . We find that the slope of the scaling curve (scaling exponent α) depends on the value of the offset a . (b) Dependence of the scaling exponent α on the offset a [fitting region for α is $n \in (30, 3000)$]. We observe a dramatic change from $\alpha = 1.5$ at $a \simeq 0$ to $\alpha = \ell + 1$ at $a > 0.01$, where ℓ is the order of the DFA method.

(i) We first consider the exponential function in the form: $y = \exp(cx + a)$, where $0 < x \leq 1$, $x = i/N_{max}$, $i = 1, \dots, N_{max}$, $N_{max} = 2^{17}$, the parameter $c = \pm 1$, the offset parameter a is a positive constant. We show the result of the DFA method in Fig. 5. We find that the slope of the detrended fluctuation function $F(n)$ vs. the scale n obtained from the DFA method does not depend on the values of the parameters c and a (there is only a vertical shift in $F(n)$ for different values of a and c) [Fig. 5(a)]. Instead, we find that the DFA scaling expo-

nent α depends only on the order ℓ of polynomial fit in the DFA method — $\alpha = \ell + 1$ — suggesting that the results of the DFA method do not depend on the details of the exponential function [Fig. 5(b)]. An analytic derivation for the fluctuation function $F(n)$ and the value of the scaling exponent α obtained from DFA-1 is presented in Appendix A.

(ii) We next consider the performance of the DFA method on a logarithmic function of the general form: $y = \log_{10}(x + a)$, where $0 < x \leq 1$, $x = i/N_{max}$,

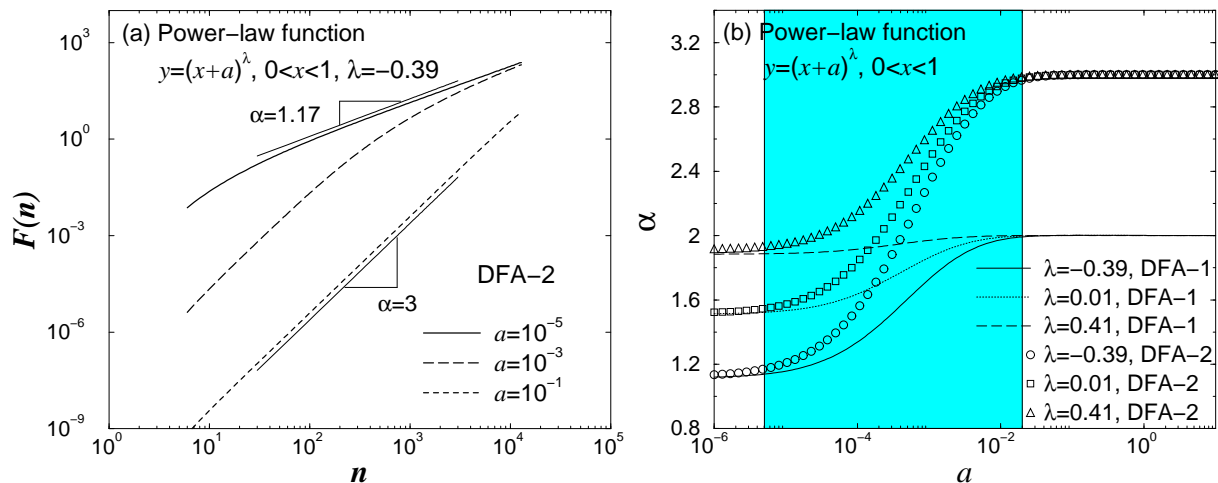


FIG. 7: The results of the DFA method for general power-law function $y = (x + a)^\lambda, 0 < x \leq 1, x = i/N_{max}, i = 1, 2, \dots, N_{max}, N_{max} = 2^{17}$, where λ is the power and the offset parameter a is a positive constant. (a) Detrended fluctuation function $F(n)$ obtained using the DFA-2 method for fixed $\lambda = -0.39$ and different values of the offset parameter a . We find that the slope of the scaling curve (scaling exponent α) depends on the value of a . (b) Dependence of the scaling exponent α on the offset a for different values of the power λ [fitting region for α is $n \in (30, 3000)$]. We observe a dramatic change from $\alpha \simeq \lambda + 1.5$ at $a \simeq 0$ for different values of λ to $\alpha = \ell + 1$ for $a > 10^{-2}$, where ℓ is the order of the DFA method.

$i = 1, \dots, N_{max}, N_{max} = 2^{17}$ and the offset parameter a is a positive constant. Specifically, we investigate the dependence of the DFA scaling exponent α on the value of the offset parameter a . We find that for very small values of a , the DFA scaling exponent is $\alpha = 1.5$. With increasing a , we observe a crossover in $F(n)$ at intermediate scales n — from $\alpha = 1.5$ at large scales to $\alpha = 3$ at small scales for DFA-2 [Fig. 6(a)]. For larger values of a , we observe a scaling behavior in $F(n)$ characterized by a single exponent $\alpha = 3$ in the entire range of scales n [Fig. 6(a)]. In Fig. 6(b) we present the dependence of the DFA scaling exponent α [obtained in the fitting range $n \in (30, 3000)$] on the offset parameter a for different DFA order ℓ . We find that for $a < 10^{-5}$ the exponent α does not depend on the order ℓ of the DFA method and takes on a single value $\alpha = 1.5$. In contrast, for large values of $a > 10^{-2}$, the exponent α depends only on the order ℓ of the DFA method and takes on values $\alpha = \ell + 1$. This behavior is identical with the behavior obtained for the exponential function in Fig. 5(b). For intermediate values of a , we observe a crossover in the scaling behavior of the fluctuation function $F(n)$ from $\alpha = 1.5$ to $\alpha = \ell + 1$.

(iii) Finally, we consider the general power-law function: $y = (x + a)^\lambda$, where $0 < x \leq 1, x = i/N_{max}, i = 1, \dots, N_{max}, N_{max} = 2^{17}$, the power λ takes on real values and the offset parameter a is a positive constant. As in the case of the logarithmic function, we find again that the DFA scaling exponent α depends on the value of the offset parameter a [Fig. 7(a)]. For certain fixed values of λ and with increasing a , we observe a gradual transition in the fluctuation function $F(n)$ from a scaling behavior spanning over a broad range of scales n characterized by a small value of the exponent α to a

crossover at intermediate scales n for larger values of a , and finally to a scaling spanning over all scales n with exponent $\alpha = 3$ for large values of a for DFA-2. In a previous study [10] we have found a specific relationship between the DFA exponent α and the value of the power λ for the case of power-law function with offset parameter $a = 0$: $\alpha = \ell + 1$ for $\lambda > \ell - 0.5$; $\alpha \simeq \lambda + 1.5$ for $-1.5 < \lambda < \ell - 0.5$; $\alpha = 0$ for $\lambda < -1.5$, where ℓ is the order of polynomial fit in the DFA- ℓ method. Our current analysis shows that this behavior is even more complicated when $a > 0$ [Fig. 7(b)]. Specifically, we find that for values of $a < 10^{-5}$ the scaling exponent α [obtained in the fitting range $n \in (30, 3000)$] depends only on the value of the power λ : $\alpha \simeq \lambda + 1.5$. In contrast, for large values of the offset parameter $a > 10^{-2}$, we find that the exponent α depends only on the order ℓ of the DFA method, and takes on values $\alpha = \ell + 1$, which is similar to the results obtained for the general exponential and logarithmic functions in this range of a [Fig. 5(b) and Fig. 6(b)]. For intermediate values of a and for $-1.5 < \lambda < \ell - 0.5$, we observe a crossover in the scaling behavior of the fluctuation function $F(n)$ from $\alpha \simeq \lambda + 1.5$ to $\alpha = \ell + 1$. Further, we find that for $\lambda > \ell - 0.5$, the DFA- ℓ scaling exponent remains constant $\alpha = \ell + 1$, and does not depend on the values of the offset parameter a — we note that for $\lambda = 0.41$ (close to $\lambda = 0.5 = \ell - 0.5$ for DFA-1) the dependence of α on a is close to a horizontal line [Fig. 7(b)].

Analytic arguments

Our results show that for large values of the offset parameter a , the detrended fluctuation function $F(n)$ for all three analytic functions — exponential, logarithmic, and power-law — exhibits identical slope, where the DFA scaling exponent α does not depend on the particular

functional form but only the order ℓ of the DFA method: $\alpha = \ell + 1$ [Fig. 5(b), 6(b) and 7(b)]. The reason for this common behavior is that (i) for large values of a , in each DFA box of a given length n , all three functions can be expanded in converging Taylor series, allowing for a perfect fit by a finite order polynomial function, and (ii) that, due to this convergence, the same polynomial function can be used when shrinking the box length n . In contrast, for very small values of the offset parameter a , the DFA results for all three functions are distinctly different and does not depend on the order ℓ of the DFA method. Below we give some general analytic arguments for the dependence of the DFA exponent α on the offset parameter a presented in Figs. 5, 6 and 7.

(i) *General exponential function:* $y = \exp(x+a), 0 < x \leq 1$.

First, we substitute the variable x by $z = x + a$: $y = e^z, z \in (a, 1 + a]$. Next, we consider a DFA box starting at the coordinate $z' = s$ and ending at $z'' = s + t$, where t is proportional to the number of points n in the box — $t = (1 + a - a)n/N_{max} = n/N_{max}$. For any value of $z \in (s, s + t)$ we can expand the function in a Taylor series:

$$e^z = \exp(s + z_0)|_{0 < z_0 < t} = e^s \left[1 + z_0 + \frac{z_0^2}{2!} + \dots \right]. \quad (1)$$

Since this expansion converges, a finite polynomial function can accurately approximate the exponential function in each DFA box. We note that the DFA- ℓ method applied to above polynomial functions gives the scaling exponent $\alpha = \ell + 1$ (see [10]). Thus, for any exponential function we find that the DFA scaling does not depend on the value of the offset parameter a and depends only on the order ℓ of the polynomial fit in the DFA- ℓ procedure [Fig. 5(b)].

(ii) *General logarithmic function:* $y = \log_{10}(x + a), 0 < x \leq 1$.

First, we substitute the variable x by $z = x + a$: $y = \log_{10}(z), z \in (a, 1 + a]$. Next, we consider a DFA box starting at the coordinate $z' = s$ and ending at $z'' = s + t$, where t is proportional to the number of points n in the box — $t = n/N_{max}$. For any value of $z \in (s, s + t)$ the Taylor expansion is:

$$\begin{aligned} \log_{10}(z) &= \log_{10}(s + z_0)|_{0 < z_0 < t} \\ &\sim \ln(1 + z_0/s) \\ &= \frac{z_0}{s} - \frac{1}{2} \left(\frac{z_0}{s}\right)^2 + \dots \frac{(-1)^{m-1}}{m} \left(\frac{z_0}{s}\right)^m + \dots \end{aligned} \quad (2)$$

This series is converging only when $z_0/s < 1$, i.e., $z_0 < s$. Since $z_0 \in (0, t)$, the condition for convergence in any DFA box $(s, s + t)$ partitioning the function is $t < s$. From $t = n/N_{max}$ and $s \in [a, 1 + a - t]$, we find that if $a > n/N_{max}$, the logarithmic function in all DFA boxes is converging, and thus each box can be approximated

by a polynomial function, leading to scaling exponent $\alpha = \ell + 1$ — depending only on the order ℓ of the DFA- ℓ method [Fig. 6].

When $t > s$, for certain values of $z_0 \in (0, t)$, the series in Eq. (2) is diverging. Since $s \in [a, 1 + a - t]$, for $s = a < t = n/N_{max}$, we find that the logarithmic function is divergent in the first DFA box $(a, a + t)$, leading to deviation in the DFA scaling for small values of a [Fig. 6].

(iii) *General power-law function:* $y = (x + a)^\lambda, x \in (0, 1]$.

First, we substitute the variable x by $z = x + a$: $y = z^\lambda, z \in (a, 1 + a]$. Next, we consider a DFA box starting at the coordinate $z' = s$ and ending at $z'' = s + t$, where t is proportional to the number of points n in the box — $t = n/N_{max}$. For any value of $z \in (s, s + t)$ the Taylor expansion is:

$$\begin{aligned} z^\lambda &= (s + z_0)^\lambda|_{0 < z_0 < t} \\ &\sim \left(1 + \frac{z_0}{s}\right)^\lambda \\ &= 1 + \lambda \frac{z_0}{s} + \frac{\lambda(\lambda - 1)}{2!} \left(\frac{z_0}{s}\right)^2 + \dots \end{aligned} \quad (3)$$

Similar to the case of the logarithmic function, this series is converging only when $z_0/s < 1$. Following the same arguments as for the logarithmic function we find that when $a > n/N_{max}$, the power-law function is converging in any DFA box, and thus can be approximated by a polynomial function, leading to the scaling exponent $\alpha = \ell + 1$ [Fig. 7], which is identical to the case of exponential and logarithmic function.

In contrast, for $a < n/N_{max}$, the power-law function is divergent in the first DFA box $(a, a + t)$, as in the case of the logarithmic function, leading to a deviation in the scaling of $F(n)$ for small values of a [Fig. 7]. While in the case of logarithmic function this divergence leads to a fixed scaling exponent $\alpha = 1.5$, for power-law functions the value of the scaling exponent α depends also on the power λ [Fig. 7].

We note that the above arguments can be used to estimate the results of the DFA method for other functions. For all functions which can be expanded in convergent Taylor expansion of a polynomial form in each DFA box partitioning the function, the DFA method leads to identical scaling results with the exponent $\alpha = \ell + 1$, which is a notable inherent limitation of the method. When there is divergent behavior in some or all of the DFA boxes partitioning a function, the DFA scaling exhibits crossover behavior to different values of the scaling exponent α which depends on the functional form and the specific parameters of the function.

VI. CONCLUSIONS

In summary, our study shows that linear transforms do not change the scaling properties of a signal. However,

the correlation properties of a signal change after applying a polynomial filter. Moreover, such change depends on the type of correlations (positive or anti-correlations) in the signal, as well as on the power (odd or even) of the polynomial filter. For the logarithmic filter we find that the scaling behavior of the transformed signal remains unchanged only when the original signal satisfies certain type of correlations (characterized by scaling exponent within a given range). Comparing the “apparent” scaling behavior of the exponential, logarithmic, and power-law functions we find that within certain range for the values of the parameters, the DFA fluctuation function $F(n)$ exhibits an identical slope, and that the DFA results of a class of other analytic functions can be reduced to these three cases. We attribute this behavior to specific limitations of the DFA method. Therefore, careful tests are necessary to accurately estimate the correlation properties of signals after nonlinear transforms.

Acknowledgments

This work was supported by NIH Grant HL071972 and NIH/National Center for Research Resources (Grant No. P41RR13622) and by the Spanish Ministerio de Ciencia y Tecnología (grants BFM2002-00183 and BIO2002-04014-CO3-02).

APPENDIX A: DFA-1 IN EXPONENTIAL FUNCTIONS

We consider an exponential function of the type $\exp(cx + a)$, where the parameters c and a take on real

values. The first step of the DFA method is to integrate the signal [Sec.II]:

$$\int_0^x \exp\left(\frac{cy}{N} + a\right) dy = N \frac{e^{\frac{cx}{N} + a} - e^a}{c}, \quad (\text{A1})$$

where N is the length of the signal and $x \in (0, N]$. We divide the variable in the exponential by N , so that (x/N) is in the interval $(0, 1]$, as considered in Sec. V. The next step of the DFA method is to divide the integrated signal into boxes of length n . For DFA-1, the squared detrended fluctuation function in the k -th box, $F^2(n, k)$, is

$$F^2(n, k) = \frac{1}{n} \int_{(k-1)n}^{kn} \left[N \frac{e^{\frac{cx}{N} + a} - e^a}{c} - (b_k x - d_k) \right]^2 dx, \quad (\text{A2})$$

where the parameters b_k and d_k are obtained by a linear fit to the integrated signal using least squares in the k -th box. These two parameters can be obtained analytically, although their expressions are too long. To obtain the squared detrended fluctuation function for the entire signal partitioned in non-overlapping boxes of length n , we sum over all boxes and calculate the average value:

$$F^2(n) = \frac{1}{N/n} \sum_{k=1}^{N/n} F^2(n, k) = \frac{1}{N/n} \sum_{k=1}^{N/n} \frac{1}{n} \int_{(k-1)n}^{kn} \left[N \frac{e^{\frac{cx}{N} + a} - e^a}{c} - (b_k x - d_k) \right]^2 dx. \quad (\text{A3})$$

Here, the index k in the sum ranges from 1 to N/n (there are N/n boxes of length n in the signal of length N). Using the analytical expressions for b_k and d_k , $F^2(n)$ can be presented analytically in the form:

$$F^2(n) = g(n) \cdot h(n), \quad (\text{A4})$$

where

$$g(n) = \left\{ -8Nc^2n^2 \left(1 + e^{\frac{cn}{N}} + e^{\frac{2cn}{N}} \right) + c^3n^3 \left(e^{\frac{2cn}{N}} - 1 \right) + 24N^2 \left[- \left(e^{\frac{cn}{N}} - 1 \right)^2 N - cn + cne^{\frac{2cn}{N}} \right] \right\} \quad (\text{A5})$$

and

$$h(n) = \frac{e^{2a} (e^{2c} - 1) N^2}{2c^6 \left(e^{\frac{2cn}{N}} - 1 \right) n^3}. \quad (\text{A6})$$

Due to the complexity of $g(n)$ and $h(n)$, the expression

of $F^2(n)$ is very complicated. However, as $n < N$ (and usually, $n \ll N$), one can expand $F^2(n)$ in powers of n to obtain:

$$F^2(n) \simeq \frac{c(e^{2c} - 1)e^{2a}}{1440N^2}n^4. \quad (\text{A7})$$

Finally, for the detrended fluctuation function $F(n)$ we obtain:

$$F(n) \simeq \sqrt{\frac{c(e^{2c} - 1)e^a}{1440}} \frac{n^2}{N}. \quad (\text{A8})$$

Thus the DFA-1 scaling exponent is $\alpha = 2$ (in agreement with the numerical simulation in Sec. V, Fig. 5). In general, we can obtain in a similar way that $\alpha = \ell + 1$, when DFA- ℓ with an order ℓ of polynomial fit is used.

-
- [1] R. L. Stratonovich, *Topics in the Theory of Random Noise Vol. 1* (Gordon & Breach, New York, 1981).
- [2] H. E. Hurst, Trans. Am. Soc. Civ. Eng. **116**, 770 (1951).
- [3] B. B. Mandelbrot and J. R. Wallis, Water Resources Res. **5**, No. 2, 321 (1969).
- [4] C.-K. Peng, S. V. Buldyrev, S. Havlin, M. Simons, H. E. Stanley, and A. L. Goldberger, Phys. Rev. E **49**, 1685 (1994).
- [5] M. S. Taqqu, V. Teverovsky, and W. Willinger, Fractals **3**, 785 (1995).
- [6] C.-K. Peng, S. V. Buldyrev, A. L. Goldberger, S. Havlin, M. Simons, and H. E. Stanley, Phys. Rev. E **47**, 3730 (1993).
- [7] S. M. Ossadnik, S. B. Buldyrev, A. L. Goldberger, S. Havlin, R. N. Mantegna, C.-K. Peng, M. Simons, and H. E. Stanley, Biophys. J. **67**, 64 (1994).
- [8] G. M. Viswanatha, C.-K. Peng, H. E. Stanley, and A. L. Goldberger, Phys. Rev. E **55**, 845 (1997).
- [9] J. W. Kantelhardt, E. Koscielny-Bunde, H. H. A. Rego, S. Havlin, and A. Bunde, Physica A **295**, 441 (2001).
- [10] K. Hu, P. Ch. Ivanov, Z. Chen, P. Carpena and H. E. Stanley, Phys. Rev. E **64**, 011114 (2001).
- [11] R. N. Mantegna, S. V. Buldyrev, A. L. Goldberger, S. Havlin, C.-K. Peng, M. Simons, and H. E. Stanley, Phys. Rev. Lett. **73**, 3169 (1994).
- [12] R. N. Mantegna, S. V. Buldyrev, A. L. Goldberger, S. Havlin, C.-K. Peng, M. Simons, and H. E. Stanley, Phys. Rev. Lett. **76**, 1979 (1996).
- [13] P. Carpena, P. Bernaola-Galván, P. Ch. Ivanov, and H. E. Stanley, Nature (London) **418**, 955 (2002).
- [14] K. K. L. Ho, G. B. Moody, C.-K. Peng, J. E. Mietus, M. G. Larson, D. Levy, and A. L. Goldberger, Circulation **96**, 842 (1997).
- [15] P. Ch. Ivanov, A. Bunde, L. A. Nunes Amaral, S. Havlin, J. Fritsch-Yelle, R. M. Baevsky, H. E. Stanley, and A. L. Goldberger, Europhys. Lett. **48**, 594 (1999).
- [16] S. M. Pikkujamsa, T. H. Makikallio, L. B. Sourander, I. J. Raiha, P. Puukka, J. Skytta, C.-K. Peng, A. L. Goldberger, and H. V. Huikuri, Circulation **100**, 393 (1999).
- [17] S. Havlin, S. V. Buldyrev, A. Bunde, A. L. Goldberger, P. Ch. Ivanov, C.-K. Peng, and H. E. Stanley, Physica A **273**, 46 (1999).
- [18] H. E. Stanley, L. A. Nunes Amaral, A. L. Goldberger, S. Havlin, P. Ch. Ivanov, and C.-K. Peng, Physica A **270**, 309 (1999).
- [19] P. Ch. Ivanov, L. A. Nunes Amaral, A. L. Goldberger, and H. E. Stanley, Europhys. Lett. **43**, 363 (1998).
- [20] P. A. Absil, R. Sepulchre, A. Bilge, and P. Gerard, Physica A **272**, 235 (1999).
- [21] K. Hu, P. Ch. Ivanov, M. F. Hilton, Z. Chen, R. T. Ayers, H. E. Stanley and S. A. Shea, Proc. Natl. Acad. Sci. U.S.A. **101**, 18223 (2004).
- [22] D. Toweill, K. Sonnenthal, B. Kimberly, S. Lai, and B. Goldstein, Crit. Care Med. **28**, 2051 (2000).
- [23] A. Bunde, S. Havlin, J. W. Kantelhardt, T. Penzel, J. H. Peter, and K. Voigt, Phys. Rev. Lett. **85**, 3736 (2000).
- [24] T. T. Laitio, H. V. Huikuri, E. S. H. Kentala, T. H. Makikallio, J. R. Jalonen, H. Helenius, K. Sariola-Heinonen, S. Yli-Mayry, and H. Scheinin, Anesthesiology **93**, 69 (2000).
- [25] Y. Ashkenazy, P. Ch. Ivanov, S. Havlin, C.-K. Peng, A. L. Goldberger, and H. E. Stanley, Phys. Rev. Lett. **86**, 1900 (2001).
- [26] P. Ch. Ivanov, L. A. Nunes Amaral, A. L. Goldberger, M. G. Rosenblum, H. E. Stanley, and Z. R. Struzik, Chaos **11**, 641 (2001).
- [27] J. W. Kantelhardt, Y. Ashkenazy, P. Ch. Ivanov, A. Bunde, S. Havlin, T. Penzel, J.-H. Peter, and H. E. Stanley, Phys. Rev. E **65**, 051908 (2002).
- [28] R. Karasik, N. Sapir, Y. Ashkenazy, P. Ch. Ivanov, I. Dvir, P. Lavie, and S. Havlin, Phys. Rev. E **66**, 062902 (2002).
- [29] J. C. Echeverria, M. S. Woolfson, J. A. Crowe, B. R. Hayes-Gill, G. D. H. Croaker, and H. Vyas, Chaos **13**, 467 (2003).
- [30] J. W. Kantelhardt, S. Havlin, and P. Ch. Ivanov, Europhys. Lett. **62**, 147 (2003).
- [31] P. A. Robinson, Phys. Rev. E **67**, 032902 (2003).
- [32] K. Hu, P. Ch. Ivanov, Z. Chen, M. F. Hilton, H. E. Stanley, and S. A. Shea, Physica A **337**, 307 (2004).
- [33] J. M. Hausdorff, C.-K. Peng, Z. Ladin, J. Wei, and A. L. Goldberger, J. Applied Physiol. **78**, 349 (1995).
- [34] J. M. Hausdorff, Y. Ashkenazy, C.-K. Peng, P. Ch. Ivanov, H. E. Stanley, and A. L. Goldberger Physica A **302**, 138 (2001).
- [35] Y. Ashkenazy, J. M. Hausdorff, P. Ch. Ivanov, and H. E. Stanley, Physica A **316**, 662 (2002).
- [36] N. Scafetta, L. Griffin, and B. J. West, Physica A **328**, 561 (2003).
- [37] B. J. West and N. Scafetta, Phys. Rev. E **67**, 051917

- (2003).
- [38] K. Ivanova and M. Ausloos, *Physica A* **274**, 349 (1999).
- [39] K. Ivanova, T. P. Ackerman, E. E. Clothiaux, P. Ch. Ivanov, H. E. Stanley, and M. Ausloos, *J. Geophys. Res.* **108**,4268 (2003).
- [40] E. Koscielny-Bunde, A. Bunde, S. Havlin, H. E. Roman, Y. Goldreich, and H. J. Schellnhuber, *Phys. Rev. Lett.* **81**, 729 (1998).
- [41] P. Talkner and R. O. Weber, *Phys. Rev. E* **62**, 150 (2000).
- [42] A. Kiraly and I. M. Janosi, *Phys. Rev. E* **65**, 051102 (2002).
- [43] J. F. Eichner, E. Koscielny-Bunde, A. Bunde, S. Havlin, and H. J. Schellnhuber, *Phys. Rev. E* **68**, 046133 (2003).
- [44] K. Fraedrich and R. Blender, *Phys. Rev. Lett.* **90**, 108501 (2003).
- [45] M. Pattantyus-Abraham, A. Kiraly, and I. M. Janosi, *Phys. Rev. E* **69**, 021110 (2004).
- [46] A. Montanari, R. Rosso, and M. S. Taqqu, *Water Resour. Res.* **36**, (5) 1249 (2000).
- [47] C. Matsoukas, S. Islam, and I. Rodriguez-Iturbe, *J. Geophys. Res., [Atmos.]* **105**, 29165 (2000).
- [48] Z. Siwy, M. Ausloos, and K. Ivanova, *Phys. Rev. E* **65**, 031907 (2002).
- [49] P. A. Varotsos, N. V. Sarlis, and E. S. Skordas, *Phys. Rev. E* **67**, 021109 (2003).
- [50] P. A. Varotsos, N. V. Sarlis, and E. S. Skordas, *Phys. Rev. E* **68**, 031106 (2003).
- [51] M. A. Moret, G. F. Zebende, E. Nogueira, and M. G. Pereira, *Phys. Rev. E* **68**, 041104 (2003).
- [52] S. Bahar, J. W. Kantelhardt, A. Neiman, H. H. A. Rego, D. F. Russell, L. Wilkens, A. Bunde, and F. Moss, *Europhys. Lett.* **56**, 454 (2001).
- [53] H. D. Jennings, P. Ch. Ivanov, A. M. Martins, P. C. da Silva, and G. M. Vishwanathan, *Physica A* **336**, 585 (2004).
- [54] N. Vandewalle and M. Ausloos, *Phys. Rev. E* **58**, 6832 (1998).
- [55] Y. Liu, P. Gopikrishnan, P. Cizeau, M. Meyer, C.-K. Peng, and H. E. Stanley, *Phys. Rev. E* **60**, 1390 (1999).
- [56] I. M. Janosi, B. Janecsko, and I. Kondor, *Physica A* **269**, 111 (1999).
- [57] M. Ausloos, N. Vandewalle, P. Boveroux, A. Minguet, and K. Ivanova, *Physica A* **274**, 229 (1999).
- [58] M. Roberto, E. Scalas, G. Cuniberti, and M. Riani, *Physica A* **269**, 148 (1999).
- [59] P. Grau-Carles, *Physica A* **287**, 396 (2000).
- [60] M. Ausloos and K. Ivanova, *Phys. Rev. E* **63**, 047201 (2001).
- [61] M. Ausloos and K. Ivanova, *Int. J. Mod. Phys. C* **12**, 169 (2001).
- [62] Z. Chen, P. Ch. Ivanov, K. Hu, and H. E. Stanley, *Phys. Rev. E* **65**, 041107 (2002).
- [63] R. N. Mantegna and H. E. Stanley, *An Introduction to Econophysics : Correlations and Complexity in Finance* (Cambridge University Press, New York, 2000).
- [64] C.-K. Peng, S. Havlin, M. Schwartz, and H. E. Stanley, *Phys. Rev. A* **44**, 2239 (1991).
- [65] H. A. Makse, S. Havlin, M. Schwartz, and H. E. Stanley, *Phys. Rev. E* **53**, 5445 (1996).